New mixed $LiGa_{0.5}In_{0.5}Se_2$ nonlinear crystal for the mid-IR

Vitaliy Vedenyapin[a)], Ludmila Isaenko[a)], Alexander Yelisseyev[a)], Sergei Lobanov[a)], Aleksey Tyazhev[b)], Georgi Marchev[b)], Valentin Petrov[b)]

[a]Institute of Geology and Mineralogy, SB RAS, 43 Russkaya Str., 630058 Novosibirsk, Russia;
[b]Max-Born-Institute for Nonlinear Optics and Ultrafast Spectroscopy, 2A Max-Born-Str., D-12489 Berlin, Germany

ABSTRACT

$LiGaSe_2$ and $LiInSe_2$ are promising nonlinear crystals for conversion of laser radiation to the mid-IR spectral range which are transparent down to the visible and UV. We successfully grew a new mixed crystal as a solid solution in the system $LiGaSe_2$ - $LiInSe_2$, with a composition of $LiGa_{0.5}In_{0.5}Se_2$ which has the same orthorhombic structure (*mm*2) as the parent compounds ($LiGaSe_2$ and $LiInSe_2$). The new crystal is more technological with regard to the growth process in comparison with $LiGaSe_2$ and $LiInSe_2$ since its homogeneity range is broader in the phase diagram. We established that about 10% of the Li ions are found in octahedral position with coordination number of 3. The band-gap of $LiGa_{0.5}In_{0.5}Se_2$ is estimated to be 2.94 eV at room temperature. The transparency at the 0-level extends from 0.47 to 13 μm. The dispersion of the principal refractive indices was measured and Sellmeier equations were constructed. The fundamental wavelength range for the SHG process extends from 1.75 to 11.8 μm. The nonlinear coefficients of $LiGa_{0.5}In_{0.5}Se_2$ have values between those of $LiGaSe_2$ and $LiInSe_2$.

Key words: nonlinear optical crystals; ternary chalcogenides; mid-infrared

1. INTRODUCTION

The orthorhombic lithium ternary chalcogenides with the chemical formula $LiBC_2$ where B=In and Ga, C=S and Se, occupy a special position among the non-oxide nonlinear optical crystals because they are characterized by the widest band-gaps.[1-7] Thus, their main advantage consists in the possibility to pump them at rather short wavelengths (in the near-IR), without two-photon absorption, generating tunable mid-IR radiation by frequency down-conversion nonlinear optical processes. The wider band-gap, in comparison e.g. to their chalcopyrite type $AgBC_2$ analogues, also leads to increased damage threshold and relatively low refractive index dispersion in the infrared which is important for frequency conversion of short laser pulses. In addition, the thermal conductivity of the four $LiBC_2$ compounds is also higher than in the $AgBC_2$ compounds, which is an essential advantage at high average powers.

In the chalcopyrite family of nonlinear crystals $AgBC_2$, all four kinds of solid solutions have been studied but in the limit of $AgInC_2$, the birefringence is too low for phase-matching. In contrast, all four wurtzite type $LiBC_2$ compounds possess sufficient birefringence and obviously all their properties can be continuously tuned by engineering the composition. To the best of our knowledge, however, only the solid solution $LiIn(S_{1-x}Se_x)_2$ for x=0.5 has been grown previously.[8] In this work, we successfully grew for the first time crystals of $LiGa_{0.5}In_{0.5}Se_2$ (LGISe) and present here preliminary results on their basic properties. Such crystal engineering is potentially interesting because although most of the properties of the two parent compounds are quite similar, some of them are rather different: Thus, e.g. the two-photon absorption coefficient at 820 nm is <0.07 cm/GW for $LiGaSe_2$ but as large as 0.6 cm/GW for $LiInSe_2$.[3]

2. CRYSTAL GROWTH AND STRUCTURE

LGISe was obtained from the two compounds $LiInSe_2$ and $LiGaSe_2$, taken in stoichiometric ratio. The two ternary

Nonlinear Frequency Generation and Conversion: Materials, Devices, and Applications X, edited by Konstantin L. Vodopyanov, Proc. of SPIE Vol. 7917, 79171L · © 2011 SPIE
CCC code: 0277-786X/11/$18 · doi: 10.1117/12.874504

lithium selenides were first synthesized and grown by the methodology described in previous work.[2,7] The synthesis of the quaternary compound was performed in a graphite crucible located in a quartz container which was evacuated to a residual pressure of 10^{-3} Pa and then sealed off. The components were melted in a single zone furnace heated to a temperature of 1000°C for 1 h.

Single crystals of LGISe were grown by vertical gradient freezing using a modified Bridgman technique. The charge was loaded into the crucible with a seed on its bottom and then the crucible was inserted into a quartz container which was again evacuated down to 10^{-3} Pa and then sealed off. The growth container was introduced into the furnace which was heated at 100°C/h up to the melting point of the charge (830°C). After 10 h, the cooling process was started, with upwards movement of the isotherm corresponding to the crystallization temperature of LGISe. Taking into account that the axial gradient in the crystallization zone amounted to 15-30°C/cm, the actual growth rate was at 0.1 – 1 mm/day. Finally, the furnace was switched-off. The grown crystals had a diameter of 20 mm and a length up to 50 mm (Fig. 1). Their color varied from yellow to red depending on the deviation from stoichiometry.

Note that the melting temperature of the quaternary LGISe is lower than the melting temperatures of both $LiInSe_2$ and $LiGaSe_2$. For these two ternary compounds incongruent sublimation was observed at high temperatures.[9] Incongruent evaporation may lead to separation of the liquid into two layers of different composition at temperatures above the melting points of $LiBC_2$. One of the liquid phases contains solid inclusions which will be incorporated into the crystal grown. Lower synthesis and growth temperatures suppress the effect of incongruent sublimation and thus from the point of view of crystal growth, the quaternary compound seems quite promising for achieving good optical quality, Fig. 1.

Fig. 1. As-grown LGISe boule.

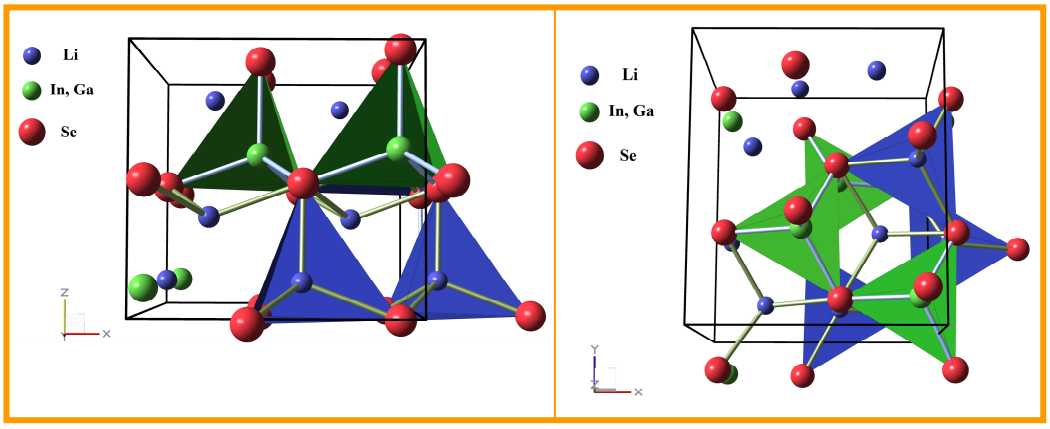

Fig. 2. $LiGa_{0.5}In_{0.5}Se_2$ possesses the same β-$NaFeO_2$ – type structure as the four ternary $LiBC_2$ compounds. However, at room temperature and normal pressure, 10% of the Li ions occupy octahedral sites.

The structure of the orthorhombic $LiBC_2$ compounds is formed by LiC_4 and BC_4 tetrahedrons, and the C-ions are arranged in hexagonal packing with tetragonal and octahedral cavities (tetrapores and octapores). The β-$NaFeO_2$ structure (space group $Pna2_1$ or C_{2v}^9) is less dense than the chalcopyrite structure of the $AgBC_2$ compounds due to the presence of these empty cavities in the unit cell volume. Only half of the tetrapores are normally occupied by Li- and B-ions while all octapores are normally empty. The crystal structure of LGISe was studied with single crystals and Oxford Diffraction Gemini R Ultra and Bruker P4 (MoK_α λ=0.71073 Å) diffractometers using the SHELXL-97 program. Two non-equivalent crystallographic positions were found for the Li-ions and about 10% of them occupy octahedral sites, Fig. 2. The same effect we confirmed also for the ternary $LiInSe_2$ but not for $LiGaSe_2$. The unit cell parameters of LGISe are a=7.0376(2) Å, b=8.3401(3) Å, and c=6.6855(2) Å. The unit cell volume is 392.4 $Å^3$, larger than in $LiGaSe_2$ and smaller than in $LiInSe_2$. In fact, assuming linear change of the lattice parameters with composition of the $LiGa_xIn_{1-x}Se_2$ solid solutions, the experimentally measured lattice parameters would correspond to a composition with x=0.42-0.43.

3. TRANSMISSION, DISPERSION AND BIREFRINGENCE

The transmission of the as-grown crystals was measured using a conventional spectrophotometer in the UV to near-IR and a Fourier-transform spectrophotometer in the mid-IR, Fig. 3a. It extends roughly from 0.47 to 13 μm at the 0-level.

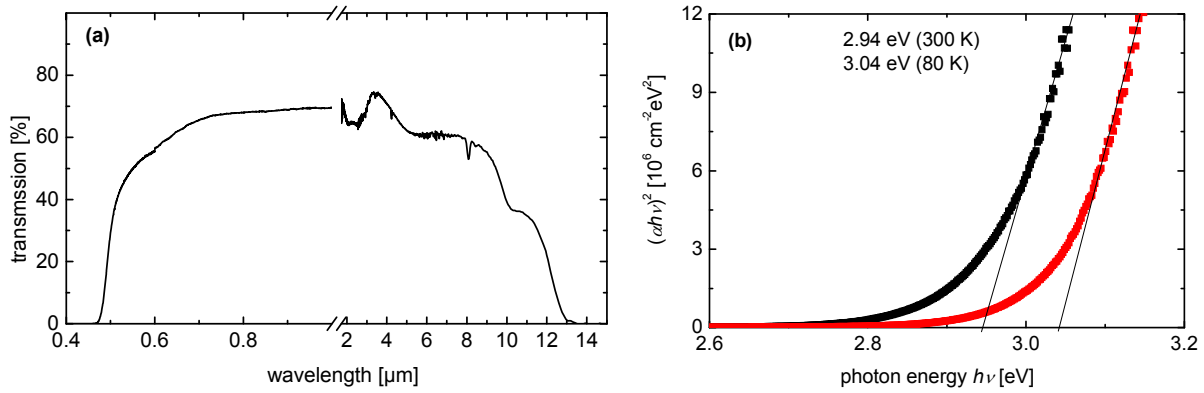

Fig. 3. (a) Unpolarized transmission measured with a 7-mm thick unoriented $LiGa_{0.5}In_{0.5}Se_2$ plate, and (b) band-gap values of $LiGa_{0.5}In_{0.5}Se_2$ estimated with a 60 μm thin unoriented plate.

The band-gap was estimated from measurements of the absorption coefficient α with a 60 μm thin plate of LGISe, Fig. 3b. From linear fits to the $(\alpha h\nu)^2$ dependence on $h\nu$ (direct allowed transitions) we arrived at 2.94 eV at 300 K which corresponds to 422 nm. For comparison, the band-gaps of $LiGaSe_2$ and $LiInSe_2$ are 3.34 and 2.86 eV, respectively.[4,6] Thus, LGISe can be pumped at 1064 nm without two-photon absorption. At 80 K, its band-gap is 3.04 eV.

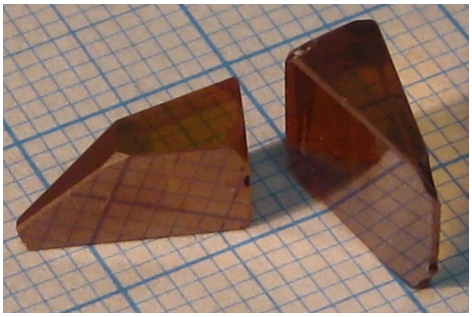

Fig. 4. Semiprisms of LGISe prepared for refractive index measurements.

From the as-grown boule of LGISe we prepared two semiprisms (Fig. 4), with the reflecting face parallel to a principal plane, for measurement of the three principal refractive indices by the autocollimation method. Table 1 shows the measured refractive indices for the 0.48-12 μm range. The data was fitted by one-pole Sellmeier equations with quadratic IR correction term. The Sellmeier coefficients are summarized in Table 2.

Table 1. Principal refractive indices of LGISe.

λ [μm]	n_x	n_y	n_z
0.48	2.49296	2.58213	2.57822
0.49	2.47908	2.56411	2.5609
0.5	2.46604	2.54903	2.54685
0.52	2.44349	2.52147	2.52025
0.54	2.42494	2.49864	2.49841
0.56	2.40866	2.47857	2.47943
0.58	2.39502	2.46254	2.46407
0.62	2.37326	2.43727	2.43904
0.66	2.3563	2.41743	2.41972
0.7	2.34361	2.4018	2.40549
0.75	2.32956	2.38583	2.38965
0.8	2.31802	2.37223	2.37631
0.9	2.30019	2.35201	2.35624
1.1	2.27994	2.32951	2.33346
1.3	2.26923	2.31722	2.32153
1.5	2.26237	2.30965	2.31395
1.7	2.25763	2.3043	2.30854
2	2.25282	2.29823	2.30321
3	2.2444	2.28956	2.29421
5	2.23495	2.27995	2.28424
7	2.22394	2.26979	2.27312
10	2.20048	2.24804	2.24948
12	2.17766	2.22733	2.22706

Table 2. Sellmeier equations for LGISe, $n^2 = A + B/(\lambda^2 - C) - D\lambda^2$ where λ is in μm, valid in the 0.48-12 μm range.

n	A	B	C	D
n_x	5.03847	0.18748	0.07033	0.00204
n_y	5.24012	0.21386	0.07977	0.00193
n_z	5.26219	0.21331	0.07550	0.00209

Figure 5a shows the measured refractive index values and the calculated curves using the fitted Sellmeier equations. Interestingly, n_y and n_z of LGISe exceed, in a substantial part of the mid-IR transmission range, the corresponding values for $LiInSe_2$ (which in turn are larger than those for $LiGaSe_2$).

The above set of Sellmeier equations predict an anomalous index crossing near 542 nm of n_y and n_z. This means that the two optic axes which determine the propagation directions where the index of refraction is independent of polarization move from the *x-z* principal plane to the *x-y* plane. Hence, the correspondence between the dielectric and

crystallographic axes in the orthorhombic LGISe is *xyz=bac* only at wavelengths above 542 nm. The angle V_z between the two optic axis and the *z*-principal optical axis, for wavelengths above 542 nm, is determined from $sinV_Z = \frac{n_Z(n_Y^2 - n_X^2)^{1/2}}{n_Y(n_Z^2 - n_X^2)^{1/2}}$.

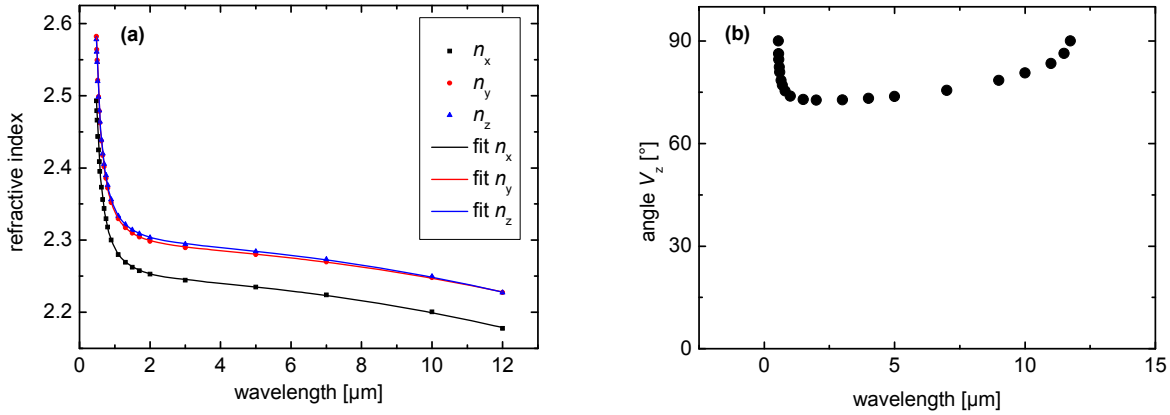

Fig. 5. (a) Experimentally measured refractive indices of LGISe (symbols) and calculated dependences (curves) using the fitted Sellmeier equations from Table 2, and (b) angle V_z between the optic axes and the principal *z*-axis of LGISe calculated by the fitted Sellmeier equations as a function of wavelength.

It is plotted in Fig. 5b. Its wavelength dependence is stronger near the index crossing point(s) but these points are close to the transparency edges where absorption is already substantial. In the interesting for practical applications clear transmission range the angle V_z is almost constant, around 75°. Thus LGISe can be considered as a negative biaxial crystal. LGISe can be obviously regarded also as quasi-uniaxial, which is a consequence of the fact that the two indices n_y and n_z are very close. Therefore no phase-matching can be expected for propagation directions in the vicinity of the *x*-principal axis.

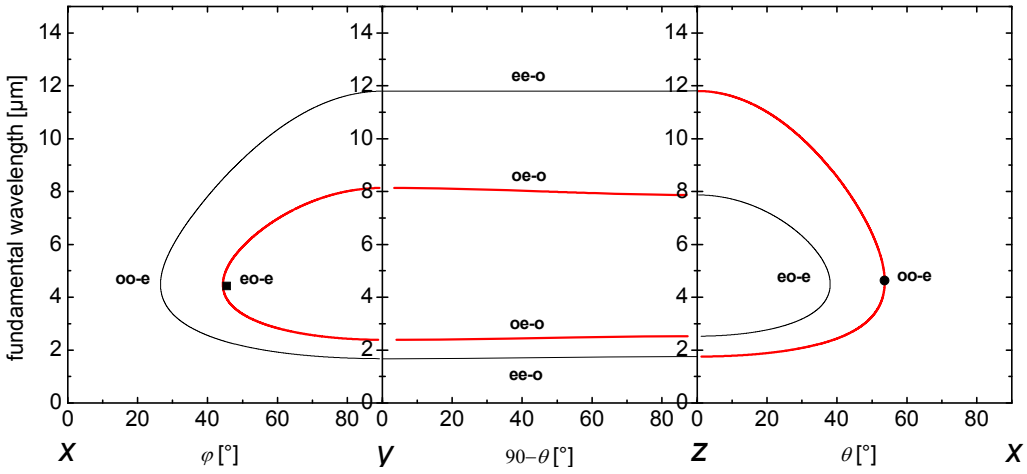

Fig. 6. SHG phase-matching in the three principal planes of LGISe. The thick red lines correspond to non-vanishing effective nonlinearity while the thin black lines, corresponding to vanishing effective nonlinearity, are given only for completeness. The symbols correspond to experimental SHG points at 4.63 μm in the *x*-*z* plane and at 4.42 μm in the *x*-*y* principal plane.

This can be seen from the second-harmonic generation (SHG) phase-matching curves calculated which are presented in Fig. 6. The figure includes all phase-matchable configurations, with non-zero and with zero effective nonlinearity. Thus, it can be easily seen that the phase-matching contours are quite symmetric, a consequence of the very close refractive indices n_y and n_z (Fig. 5a).

The predicted phase-matching angles agree very well with the SHG measurements performed in the *x*-*y* and *x*-*z* planes with femtosecond pulses. In the *x*-*z* plane the deviation at 4.63 μm was within the cut accuracy while in the *x*-*y* plane, at a fundamental wavelength of 4.42 μm, the internal experimental phase-matching angle was roughly 1° larger than the calculated one. The SHG range for the fundamental wavelength, covered by interactions in the principal planes that possess non-vanishing effective nonlinearity, extends from 1.75 to 11.8 μm.

Phase-matching for general type three-wave interactions in the *x*-*y* and *x*-*z* planes where broad tuning is combined with non-vanishing effective nonlinearity is shown in Fig. 7. The curves for type-II interaction (Fig. 7a) have two branches with opposite curvature which can cross at two points where phase-matching for the degenerate process or SHG is realized. With decreasing phase-matching angle these branches separate and a single crossing point is reached which corresponds to the single SHG solution in Fig. 6. For yet smaller angles no crossing occurs and the degeneracy point is not reached.

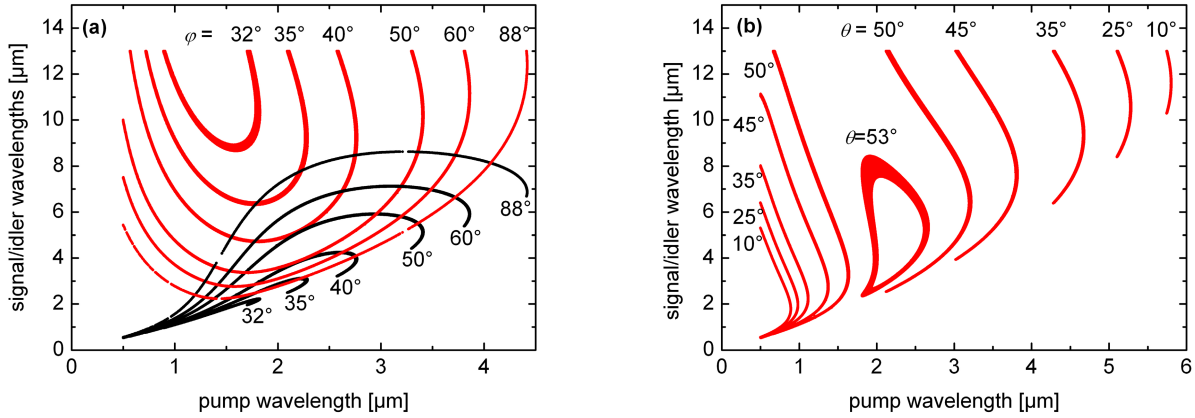

Fig. 7. Three-wave interaction phase-matching curves for LGISe: (a) eo-e phase-matching in the *x*-*y* plane and (b) oo-e phase-matching in the *x*-*z* plane.

Comparing Fig. 7a to Fig. 7b, we note that at relatively short pump wavelengths (e. g. 1064 nm) full tunability with a fixed crystal cut is achievable only in the *x*-*z* principal plane. Also, for type-I interaction in this plane two branches of the solution can be seen. Note that in the noncritical (θ=0°) configuration in this case the effective nonlinearity is zero. Increasing the phase-matching angle the two branches merge into a closed contour.

4. NONLINEAR COEFFICIENTS

In the principal planes, the expressions for the effective nonlinearity d_{eff} of LGISe read:

$$d_{eff}^{eoe} = d_{eff}^{oee} = -(d_{24}\sin^2\varphi + d_{15}\cos^2\varphi) \qquad (x\text{-}y \text{ plane}) \qquad (1a)$$

$$d_{eff}^{oeo} = d_{eff}^{eoo} = -d_{24}\sin\theta \qquad (y\text{-}z \text{ plane}) \qquad (1b)$$

$$d_{eff}^{ooe} = d_{31}\sin\theta \qquad (x\text{-}z \text{ plane}, \theta<V_Z) \qquad (1c)$$

with superscripts „*o*" and "*e*" denoting the ordinary and extraordinary beams. LGISe behaves as an optically negative uniaxial crystal in the *x*-*y* and *x*-*z* (for $\theta<V_z$) planes and as an optically positive uniaxial crystal in the *y*-*z* plane. Assuming the Kleinman symmetry condition to hold then $d_{15}=d_{31}$.

The elements d_{il} of the nonlinear tensor have been investigated by SHG using type-I or type-II interactions in the principal planes of LGISe. Since femtosecond pulses were applied for the SHG, the use of very thin oriented LGISe and reference samples makes it possible to neglect the effects of absorption, beam walk-off and focusing with the data analysis in the low-depletion limit derived from standard plane-wave SHG theory. That is why care was taken to keep the conversion efficiency low enough in order to avoid complications from saturation effects and spatial effects across the beam cross section. In the plane wave approximation and having in mind the equal fundamental energy we corrected the relative measurements only for the crystal thickness, and the slightly different index of refraction and Fresnel reflections. Unfortunately, only for type-I interaction the spectral acceptance of all three crystal samples available was much larger than the spectral bandwidth of the femtosecond pulses near 4.6 μm.

The femtosecond source at 1 kHz repetition rate was a $KNbO_3$-based optical parametric amplifier. The single pulse energy was in the 2-3 μJ range. The measurements were performed simultaneously with measurements of analogous $LiGaSe_2$ and $LiInSe_2$ samples, in order to obtain reliable information on the relative magnitute of the nonlinear coefficients.

The coefficient d_{31} was estimated by type-I SHG in the *x*-*z* plane from Eq. (1c). The LGISe sample for SHG in the *x*-*z* plane was cut at θ=53.6° and had a thickness of 0.7 mm. The reference $LiGaSe_2$ (0.9 mm thick) and $LiInSe_2$ (0.86 mm thick) samples were cut at θ=56.4° and θ=46.7°, respectively. We obtained $d_{31}(\text{LGISe})=0.94d_{31}(LiInSe_2)$ and $d_{31}(\text{LGISe})=1.03d_{31}(LiGaSe_2)$. The ratio of the nonlinear coefficients of $LiInSe_2$ and $LiGaSe_2$ was 1.1, close to the ratio of 1.19 estimated at 2.3 μm from previous measurements.[3,6] Thus, it can be concluded that within the experimental accuracy, ±10% in the relative measurements, LGISe has nonlinearities of the same order of magnitude as the other two selenide compounds. While similar measurements were performed also for type-II SHG in the *x*-*y* plane, in order to determine d_{24} from Eq. (1a), the thickness of the samples did not permit reliable estimation because the spectral acceptance was not sufficient in order to consider samples of different thickness unaffected by this factor.

5. CONCLUSION

$LiGa_{0.5}In_{0.5}Se_2$, a new quaternary nonlinear crystal for the mid-IR, was grown from the two ternary lithium chalcogenides $LiGaSe_2$ and $LiInSe_2$. The solid solution $LiGa_{0.5}In_{0.5}Se_2$ exhibits the same orthorhombic structure (*mm*2) as the parent compounds but seems more technological with regard to the growth process since its homogeneity range is broader in the phase diagram. It is transparent between 0.47 and 13 μm and the band-gap is 2.94 eV at room temperature. The Sellmeier equations, which were constructed on the basis of refractive index measurements, reproduce well SHG phase-matching angles in the principal dielectric planes. The fundamental wavelength range for the SHG process extends from 1.75 to 11.8 μm. The second-order nonlinearity of $LiGa_{0.5}In_{0.5}Se_2$ has an intermediate value, between those of $LiGaSe_2$ and $LiInSe_2$.

ACKNOWLEDGMENTS

We acknowledge support from DLR (International Bureau of BMBF) under project RUS 08/013 and from the European Community's Seventh Framework Programme FP7/2007-2011 under grant agreement n° 224042. We thank S. F. Solodovnikov for the X-ray structural analysis and V. Panyutin for the useful discussions and his help in the SHG experiments and in the preparation of this manuscript.

REFERENCES

[1] L. Isaenko, A. Yelisseyev, S. Lobanov, P. Krinitsin, V. Petrov, and J.-J. Zondy, "Ternary chalcogenides $LiBC_2$ (B=In, Ga; C=S, Se, Te) for mid-IR nonlinear optics", J. Non-Cryst. Sol. **352**, 2439-2443 (2006).

[2] J.-J. Zondy, V. Petrov, A. Yelisseyev, L. Isaenko, and S. Lobanov, "Orthorhombic crystals of lithium thioindate and selenoindate for nonlinear optics in the mid-IR," In: *Mid-Infrared Coherent Sources and Applications*, ed. by M. Ebrahim-Zadeh and I. Sorokina, NATO Science for Peace and Security Series - B: Physics and Biophysics, Springer (2008), pp. 67-104.

[3] V. Petrov, A. Yelisseyev, L. Isaenko, S. Lobanov, A. Titov, and J.-J. Zondy, "Second harmonic generation and optical parametric amplification in the mid-IR with orthorhombic biaxial crystals $LiGaS_2$ and $LiGaSe_2$," Appl. Phys. B **78**, 543-546 (2004).

[4] L. Isaenko, A. Yelisseyev, S. Lobanov, A. Titov, V. Petrov, J.-J. Zondy, P. Krinitsin, A. Merkulov, V. Vedenyapin, and J. Smirnova, "Growth and properties of $LiGaX_2$ (X=S, Se, Te) single crystals for nonlinear optical applications in the mid-IR", Cryst. Res. Technol. **38**, 379-387 (2003).

[5] S. Fossier, S. Salaün, J. Mangin, O. Bidault, I. Thenot, J.-J, Zondy, W. Chen, F. Rotermund, V. Petrov, P. Petrov, J. Henningsen, A. Yelisseyev, L. Isaenko, S. Lobanov, O. Balachninaite, G. Slekys, and V. Sirutkaitis, "Optical, vibrational, thermal, electrical, damage and phase-matching properties of lithium thioindate", J. Opt. Soc. Am B **21**, 1981-2007 (2004).

[6] V. Petrov, J.-J. Zondy, O. Bidault, L. Isaenko, V. Vedenyapin, A. Yelisseyev, W. Chen, A. Tyazhev, S. Lobanov, G. Marchev, and D. Kolker, "Optical, thermal, electrical, damage, and phase-matching properties of lithium selenoindate," J. Opt. Soc. Am. B **27**, 1902-1927 (2010).

[7] L. Isaenko, I. Vasilyeva, A. Merkulov, A. Yelisseyev, and S. Lobanov, "Growth of new nonlinear crystals $LiMX_2$ (M=Al, In, Ga; X=S, Se, Te) for the mid-IR optics," J. Cryst. Growth **275**, 217-223 (2005).

[8] Yu. M. Andreev, V. V. Atuchin, G. V. Lanskii, N. V. Pervukhina, V. V. Popov, and N. C. Trocenko, "Linear optical properties of $LiIn(S_{1-x}Se_x)_2$ crystals and tuning of phase matching conditions," Sol. State Sci. **7**, 1188-1193 (2005).

[9] L. I. Isaenko and I. G. Vasilyeva, „Nonlinear $LiB^{III}C^{VI}_2$ crystals for mid-IR and far-IR: Novel aspects in crystal growth," J. Cryst. Growth **310**, 1954-1960 (2008).